Title: Emulator-based Bayesian calibration of the CISNET colorectal cancer models.

Authors: Carlos Pineda-Antunez[1], Claudia Seguin[2], Luuk van Duuren[3], Amy B. Knudsen[2], Barak Davidi[2], Pedro Nascimento de Lima[4], Carolyn Rutter[5], Karen M. Kuntz[6], Iris Lansdorp-Vogelaar[3], Nicholson Collier[7,8], Jonathan Ozik[7,8], Fernando Alarid-Escudero[9,10]

Institutional Affiliation(s)

[1] Global Health Cost Consortium (CISIDAT), Morelos, Mexico

[2]Institute for Technology Assessment, Massachusetts General Hospital, Boston, MA, United States

[3] Department of Public Health, Erasmus MC Medical Center Rotterdam, The Netherlands

[4] RAND Corporation, Santa Monica, CA, United States

[5] Fred Hutchinson Cancer Research Center, Hutchinson Institute for Cancer Outcomes Research, Biostatistics Program, Public Health Sciences Division, Seattle WA

[6] Division of Health Policy & Management, University of Minnesota School of Public Health, Minneapolis, MN, United States

[7]Decision and Infrastructure Sciences Division, Argonne National Laboratory, Lemont, IL, United States

[8]Consortium for Advanced Science and Engineering, University of Chicago, Chicago, IL, United States

[9]Department of Health Policy, School of Medicine, Stanford University, CA, US

[10]Center for Health Policy, Freeman Spogli Institute, Stanford University, CA, US

Corresponding Author: Fernando Alarid-Escudero, Ph.D., 615 Crothers Way, #117, Encina Commons, MC 6019, Stanford, CA 94305. e-mail address: falarid@stanford.edu; phone number: +1 (650) 724-4234

Abstract

Purpose: To calibrate Cancer Intervention and Surveillance Modeling Network (CISNET) 's SimCRC, MISCAN-Colon, and CRC-SPIN simulation models of the natural history colorectal cancer (CRC) with an emulator-based Bayesian algorithm and internally validate the model-predicted outcomes to calibration targets. **Methods:** We used Latin hypercube sampling to sample up to 50,000 parameter sets for each CISNET-CRC model and generated the corresponding outputs. We trained multilayer perceptron artificial neural networks (ANN) as emulators using the input and output samples for each CISNET-CRC model. We selected ANN structures with corresponding hyperparameters (i.e., number of hidden layers, nodes, activation functions, epochs, and optimizer) that minimize the predicted mean square error on the validation sample. We implemented the ANN emulators in a probabilistic programming language and calibrated the input parameters with Hamiltonian Monte Carlo-based algorithms to obtain the joint posterior distributions of the CISNET-CRC models' parameters. We internally validated each calibrated emulator by comparing the model-predicted posterior outputs against the calibration targets. **Results:** The optimal ANN for SimCRC had four hidden layers and 360 hidden nodes, MISCAN-Colon had 4 hidden layers and 114 hidden nodes, and CRC-SPIN had one hidden layer and 140 hidden nodes. The total time for training and calibrating the emulators was 7.3, 4.0, and 0.66 hours for SimCRC, MISCAN-Colon, and CRC-SPIN, respectively. The mean of the model-predicted outputs fell within the 95% confidence intervals of the calibration targets in 98 of 110 for SimCRC, 65 of 93 for MISCAN, and 31 of 41 targets for CRC-SPIN. **Conclusions:** Using ANN emulators is a practical solution to reduce the computational burden

and complexity for Bayesian calibration of individual-level simulation models used for policy analysis, like the CISNET CRC models.

Keywords: Bayesian calibration, emulator, machine learning, artificial neural networks, colorectal cancer model

Introduction

Individual-based simulation models are often used to evaluate health policies that aim to reduce the impact of diseases (1). For many of these models, data to directly inform the parameters are lacking and often estimated through calibration. Ideally, the uncertainty in model parameters should be accurately quantified during the calibration process so that the ultimate model predictions also reflect this uncertainty (2). Therefore, the calibration process aims to obtain a joint posterior distribution of the calibrated parameters that produce model outputs consistent with the calibration targets (observed data arising from a clinical or epidemiological system) and their uncertainty (3). The complexity of these models has increased with higher availability of data and computational power, and greater model complexity often means more parameters, making calibration more challenging (4).

Bayesian methods are suitable for calibrating health decision models. They provide the posterior joint uncertainty of calibrated parameters given the prior distributions for model parameters, the structural assumptions of the model, and a likelihood function created from the calibration data (5). However, there are many challenges involved in Bayesian calibration. The computing time for calibrating complex models is significantly more extensive and demands high computational power, requiring running the model thousands or even millions of times to achieve convergence (6).

One approach to reducing the computational burden uses an emulator or metamodel that serves as a surrogate of the original complex simulation model (often referred to as a simulator) by mapping the relationship between the inputs and outputs of the simulator (7). An emulator is a proxy model that is less complex and faster than a simulator, can replace a simulator to predict outcomes, and is often used in other model-based analyses, such as sensitivity analysis (8),

calibration procedures (9), policy optimization (7,10), cost-effectiveness analysis (11), and extrapolating findings to other settings (12). Using emulators for Bayesian calibration can reduce the computational time without losing the possibility of producing outcomes that match observed data (9,13).

This work aims to quantify the uncertainty of parameters of three microsimulation models of the natural history of colorectal cancer (CRC) using Bayesian Calibration with Artificial Neural Networks (BayCANN), an emulator-based algorithm (9) and validate the model-predicted outcomes to calibration targets.

Methods

We used three models from the Cancer Intervention and Surveillance Modeling Network (CISNET) Colorectal Cancer (CRC) Working Group - Simulation Model of Colorectal Cancer (SimCRC), Microsimulation Screening Analysis (MISCAN-Colon), and Colorectal Cancer Simulated Population model for Incidence and Natural history (CRC-SPIN) –focused on the long-term objective of reducing the burden of CRC. These microsimulation models describe the natural history of CRC using different underlying structures(14). They have a long history of use in comparative modeling analyses to provide the information needed to address key policy questions and prioritize future research and have been used to evaluate various health policies and clinical strategies, such as screening and surveillance of CRC programs in the US (15,16).

Under the BayCANN algorithm, we construct ANNs as emulators replacing the CISNET CRC models for Bayesian calibration. In the following sections, we describe six steps to implement BayCANN. An illustration of the BayCANN process is shown in Figure 1.

Design of experiment

The first step in designing an emulator is obtaining a set of inputs and their corresponding output values from the original model using a design of simulation experiment (17). These input-output pairs are required to map the underlying structure of the models. We used Latin Hypercube Sampling (LHS) to generate model parameter inputs that efficiently sample the parameter space. We designed the LHS such that the sample parameter values should produce model outputs that cover the mean of the calibration targets. Poor coverage of the targets with the model outputs will prevent the emulator from producing accurate posterior distributions. In Figure S1 of the supplementary material, we show the coverage of the LHS design for the three models.

Splitting samples and rescaling inputs and outputs

For the second step, we prepare data for the emulator training. First, we split the LHS data into training and testing sets using 80% and 20% of the data, respectively, to reduce overfitting. Second, we scaled the inputs and outputs from -1 to 1 to have all the data on the same scale because different magnitudes between and within inputs and outputs could reduce the performance and efficiency of training the ANN (18).

Constructing the Artificial Neural Networks

In the third step, we build the emulator using a Multilayer Perceptron (MLP), which consists of one input layer, one or more hidden layers, and one output layer, each consisting of nodes that are all connected between layers, often referred to as a fully connected class of ANN (18) The input layer takes in the different values for each model input parameter and has as many nodes as the number of the simulator input parameters to be calibrated. The output layer contains as many nodes as the number of the simulator model outputs to be used to compare to the

calibration targets. The number of hidden layers and nodes are considered hyperparameters and are determined based on the fit of the ANN to the model outcomes.

To find the optimal hyperparameters, we performed a grid search using a full factorial design by varying the number of hidden layers between one and five and the number of hidden nodes per hidden layer starting from the number of model outputs up to 300 more with increments of 20. We selected the structure that minimizes the mean square error (MSE) on the validation set. Because each CISNET CRC model has a different number of input parameters and outcomes, we trained a separate ANN for each model. We also explored other hyperparameters, such as activation functions (sigmoidal, hyperbolic tangent, relu), batch size (500, 1000, 2000), and the optimizer (Adam, gradient descendent), to improve the performance prediction of the ANN.

Equation (1) describes the MLP ANN emulators for the three CISNET-CRC models.

$$\begin{gathered}
z^{(0,m)} = W^{(0,m)}X^{(,m)} + b^{(0,m)} \\
h^{(0,m)} = f^{(0,m)}\left(z^{(0,m)}\right) \\
z^{(1,m)} = W^{(1,m)}h^{(0,m)} + b^{(1,m)} \\
\vdots \\
z^{(l,m)} = W^{(l,m)}h^{(l-1,m)} + b^{(l,m)} \\
h^{(l,m)} = f^{(l,m)}\left(z^{(l,m)}\right) \\
z^{(l+1,m)} = W^{(l+1,m)}h^{(l,m)} + b^{(l+1,m)} \\
\vdots \\
h^{(L-1,m)} = f^{(L-1,m)}\left(z^{(L-1,m)}\right) \\
z^{(L,m)} = W^{(L,m)}h^{(L-1,m)} + b^{(L,m)} \\
Y^{(m)} = f^{(L,m)}\left(z^{(L,m)}\right)
\end{gathered} \tag{1}$$

Where $\boldsymbol{X}^{(m)} = \left(X_{1,m}, X_{2,m}, \dots, X_{I,m}\right)$ is the vector of parameters for the model $m = \{CRCSPIN, MISCANColon, SimCRC\}$, $W^{(l,m)}$ is the matrix of weights for layer $l = 0, \dots, L$, $l = 0$ is the input layer, and $l = L$ is the output layer, and $0 < l < L$ represents a hidden layer, $b^{(l,m)}$

is the vector of biases in layer l, $z^{(l,m)}$ is the weighted sum of inputs to the nodes in layer l, and $f^{(l,m)}$ is the activation function in layer l. An activation function on layer l aggregates a non-linear relationship between layers $(l-1)$ and l. $h^{(l,m)}$is the activation function evaluated in $z^{(l,m)}$, which is the input for the nodes in the next layer. Finally, $Y^{(m)} = \left(Y_{1,m}, Y_{2,m}, \dots, Y_{O,m}\right)$ is the vector of predicted-emulator outcomes for model *m*.

We evaluated the goodness of fit of the emulators in reproducing the CISNET-CRC model-predicted outcomes by estimating the average R-square between each pair of emulators and simulator output in the LHS test sample(19).

Bayesian calibration

In the fourth step, we implemented the selected ANN structure for each CRC model by coding their equation in Stan (Stan Development Team, 2022). In this step, the emulators replaced the CRC models within the Bayesian calibration algorithm. Using four Hamiltonian Monte Carlo chains, we drew 100,000 samples from the posterior distribution. We verified the mixing and convergence of the chains using the R-hat convergence diagnostic. If chains have not mixed well, the R-hat is greater than 1.

Rescaling posterior distribution to original input parameter scale

In the fifth step, after obtaining the posterior distributions using the emulator, we transformed the inputs back to the original scale to use them in the corresponding CISNET model to validate that the model outputs fit their related calibration targets.

Internal validation

Lastly, in the sixth step, we internally validated each calibrated simulator using a Bayesian posterior predictive check by propagating the uncertainty of the posterior parameter distributions on model-predicted outputs. We drew a sample of 1,000 sets of calibrated

parameters from BayCANN and ran each of the CISNET-CRC models for each set to produce their corresponding outputs that we subsequently compared to the calibration targets. We verified that the mean values of the model-predicted outputs fall within the calibration target uncertainty defined as the 95% confidence interval for each target.

Results

Inputs and outputs from the simulation models

Using an LHS design, we sampled 50,000, 37,000, and 16,900 parameter sets and generated corresponding outputs for the SimCRC, MISCAN-Colon, and CRC-SPIN models, respectively, using the Argonne Leadership Computing Facility (ALCF) Theta supercomputer. The time the models took for each run was 3.8, 5.0, and 5.6 minutes/core for the CRC-SPIN, MISCAN-Colon, and SimCRC models, respectively. The models varied in terms of the coverage of the calibration targets. SimCRC covered 100% of the targets, MISCAN-Colon covered 94% and CRCSPIN covered 85%. The targets' coverage for each CISNET-CRC model is shown in Figure S1 in the supplementary material.

ANN emulators of CISNET-CRC models

The number of hidden layers and nodes from the ANN structure with the lowest MSE varied across models. SimCRC's ANN had four hidden layers with 360 hidden nodes, MISCAN-Colon's ANN had four hidden layers with 114 hidden nodes, and CRC-SPIN's ANN had one hidden layer with 140 hidden nodes. The computer used for emulator training had 8 cores and 32 GB RAM. The duration of training varied for different models, with 39, 26, and 10 minutes taken for SimCRC, MISCAN-Colon, and CRC-SPIN, respectively, as shown in Table 1. The training time was influenced by the structure of the ANNs as well as the number of samples

utilized in each LHS design. The more hidden nodes or layers and the more samples to train, the longer it took to train them.

We obtained goodness of fit in terms of the average R-squared of 0.987, 0.997, and 0.899 for SimCRC, MISCAN-Colon, and CRC-SPIN emulators, respectively. Figure 2 shows the prediction performance of the three emulators, where each point is the pair of CISNET-CRC model (X-axis) and emulator prediction (Y-axis) of a sample of CRC incidence targets for a given parameter set in the LHS, and the 45º line means a perfect prediction. For this sample of incidence outputs, the MISCAN-Colon emulator had the best performance of all the emulators.

Bayesian convergence diagnostics

We used the final ANN emulators and implemented them in Stan to obtain the calibrated posterior distributions of the parameters using four independent chains. For all three CISNET-CRC emulators, we obtained good convergence and mixing for the four chains of the posterior distribution with an R-hat less than 1.003 for all parameters of the three CISNET-CRC models. Values of the R-hat smaller than 1.2 have been set as thresholds for satisfactory convergence (21). Additional diagnostics of the Bayesian calibration, such as R-hat (for convergence) and Effective Sample Size (for efficiency), are shown in Figure S2 in the supplementary material. Most of the parameters' chain correlation converged to zero after the first iterations, which is also an indicator of good mixing on MCMC chains. The calibration process was conducted on the same computer used to train the emulators, and the time required to calibrate the emulators differed by model, with longer times for models with more inputs and outputs. The times for calibrating the emulator were 6.7, 3.6, and 0.5 hours for SimCRC, MISCAN-Colon, and CRC-SPIN, respectively.

Calibrated posterior distributions

After the calibration, the posterior distribution of the calibrated parameters shrunk compared to the prior distributions. The level of shrinkage varied between the models. For example, Figure 3 illustrates that the *hazard_mean_uk* parameter in the MISCAN-Colon model showed a more pronounced shrinkage than *pSxDetS1_D* and *growth.rectum.beta1* parameters in SimCRC and CRC-SPIN parameters, respectively. In general, most of the posterior distributions shrunk compared to their priors. The prior and posterior marginal distributions for all model parameters are shown in Figure S3 in the supplementary material.

The posterior distribution for MISCAN-Colon had the highest correlation values reaching 0.99, followed by SimCRC with 0.93 and 0.74 for CRC-SPIN. The joint posterior distributions of all pairwise parameters for the three CISNET-CRC models are shown in Figure S4 in the supplementary material. Highly correlated parameters are often found in these types of simulation models with a high number of parameters (2)

Internal validation

The calibrated models showed good internal validation. Specifically, the interquartile range of the predictions of adenoma prevalence was within the target interval for all age groups in the three CISNET-CRC models. Moreover, the CRC incidence predictions were within the target interval for most age groups, as depicted in Figure 4. Overall, the mean predicted outcomes that fell within the 95% confidence intervals of the calibration targets for SimCRC were 98 of 110, 65 of 93 for MISCAN, and 31 of 41 for CRC-SPIN (see Figure S5 in the supplementary material).

Discussion

In this manuscript, we used ANN emulators of the CISNET-CRC models as a practical solution to reduce the computational burden of calibration and efficiently calibrate these models under a Bayesian framework. Although emulators have been used widely in other science and engineering areas, they have been underused in health decision science. This may be due to a lack of material and guidance on developing and validating them (22). To address these issues, we provided step-by-step guidance on constructing ANN emulators to calibrate three realistic CRC microsimulation models using a Bayesian approach. We showed that BayCANN serves as a flexible framework for building a suitable emulator for CISNET models that avoids the need to try multiple emulator alternatives, such as Gaussian process regression, generalized additive models, symbolic regression, etc., that also can be suitable metamodels but require more trial and error and consequently investing more time.

As in previous studies, our emulators proved to be an efficient alternative for conducting analysis based on complex microsimulation models and enabling computationally intensive processes such as Bayesian calibrations (7,23). The emulator-based Bayesian calibration conducted in this work provides a fast solution to calibrate multitarget models and obtain uncertainty of the model parameters. Using emulators instead of the original simulation models allowed us to perform significantly more iterations in the calibration process, which helped to improve the results. Our results showed a good calibration performance for the three CISNET-CRC models, generating outputs within targets' uncertainty for most of their outcomes (>70%). Despite the difference between the CISNET models, their ANN emulators did not vary drastically in the number of hidden layers and nodes.

ANNs showed good performance in emulating the CISNET-CRC microsimulation models, despite having many input parameters and outputs, which could be a limitation for other emulator alternatives such as Gaussian processes (7,8). We used the models with many parameters and outcomes for this work to show an application with structurally complex models that have been used to inform screening and treatment strategies. Furthermore, ANNs are relatively easy to construct in commonly used programming languages and implement in Bayesian software, such as JAGS or Stan, for calibration purposes. For these reasons, ANNs are good candidates as emulators for Bayesian calibration.

Our findings are subject to the limitations of emulators. Determining the ANN's hyperparameter values a priori can be challenging and requires some supervision in the training process. For example, we need to define the number of hidden layers and nodes, which must be sufficiently high to capture the underlying functions but not so high as to cause overfitting, which is not ideal. We split the LHS sample into training and testing sets to prevent overfitting. The testing sets were used to validate the predictions not used in the training process. We limited our search space for ANN hyperparameters and did not get prediction accuracy close to 100%; however, achieving such high accuracy levels would likely require more computational time and burden, diminishing the benefits of using emulators.

The reduced computational burden does not consider the time spent on LHS design, which is considerable given that the original individual-level models are required for this process. But, even for Bayesian calibrations that do not use emulators (e.g., IMIS), these experiment designs are often required. The number of LHS observations required to train the emulators depends on the underlying functions of each microsimulation model; we did not explore the optimal number of LHS observations needed for our emulators, so we could

potentially reduce this number to decrease the time it takes to generate the LHS without affecting the learning process of the emulators. A possible extension to our approach includes implementing adaptative sampling with emulators to identify the optimal number of LHS observations; this exercise may reduce the overall calibration time (24,25).

BayCANN is a transparent and reproducible algorithm that can facilitate the Bayesian calibration of health decision models. It can be implemented in commonly used open-source software (9). Bayesian calibration typically requires many model evaluations; we performed at least 100,000 iterations within the Hamiltonian Monte Carlo algorithm for this work. Using the CISNET models that require, on average, 4 minutes per iteration (using similar computational resources) may become prohibitively expensive. BayCANN, as with other emulator-based calibration approaches, requires the original simulator only to generate the LHS design and for internal validation. The actual Bayesian calibration is done with the trained emulator using the LHS samples. An advantage is that it is not required to code the simulator in probabilistic software (e.g. Stan), which represents another time-consuming task to perform the calibration. BayCANN can be applied to calibrate other computationally intensive individual-level decision models and contribute to the availability of algorithms that facilitate the implementation of Bayesian calibration.

Conclusion

In this study, we showed that ANNs are suitable emulators of the CISNET CRC models for Bayesian calibration. The use of emulators significantly reduced the time and computational burden for calibration. Analysts wanting to calibrate computationally-expensive simulation models to quantify calibrated parameter uncertainty accurately under a Bayesian framework could benefit from using BayCANN.

Acknowledgments:

Financial support for this study was provided by the grant U01-CA253913 from the National Cancer Institute (NCI) as part of the Cancer Intervention and Surveillance Modeling Network (CISNET). The content is solely the responsibility of the authors and does not necessarily represent the official views of the National Institutes of Health. The funding agencies had no role in the design of the study, interpretation of results, or writing of the manuscript. The funding agreement ensured the authors' independence in designing the study, interpreting the data, writing, and publishing the report. This research was completed with resources provided by the Argonne Leadership Computing Facility (Theta), which is a DOE Office of Science User Facility supported under Contract DE-AC0206CH11357.

Declarations:

All authors have read and approved the manuscript and agree with its submission to medRxiv. The authors have no conflicts of interest to declare.

References

1. Zhang X. Application of discrete event simulation in health care: A systematic review. BMC Health Serv Res. 2018 Sep 4;18(1).
2. Alarid-Escudero F, Knudsen AB, Ozik J, Collier N, Kuntz KM. Characterization and Valuation of the Uncertainty of Calibrated Parameters in Microsimulation Decision Models. Front Physiol. 2022 May 9;13.
3. Alarid-Escudero F, MacLehose RF, Peralta Y, Kuntz KM, Enns EA. Nonidentifiability in Model Calibration and Implications for Medical Decision Making. Medical Decision Making. 2018 Oct 1;38(7):810–21.
4. Sun NZ, Sun A. Model calibration and parameter estimation: For environmental and water resource systems. Model Calibration and Parameter Estimation: For Environmental and Water Resource Systems. Springer New York; 2015. 1–6621 p.
5. Menzies NA, Soeteman DI, Pandya A, Kim JJ. Bayesian Methods for Calibrating Health Policy Models: A Tutorial. Pharmacoeconomics. 2017 Jun 1;35(6):613–24.
6. Rutter CM, Miglioretti DL, Savarino JE. Bayesian calibration of microsimulation models. J Am Stat Assoc. 2009 Dec;104(488):1338–50.
7. Zhong H, Brandeau ML, Yazdi GE, Wang J, Nolen S, Hagan L, et al. Metamodeling for Policy Simulations with Multivariate Outcomes. Medical Decision Making. 2022 Jun 23;0272989X2211050.
8. de Carvalho TM, van Rosmalen J, Wolff HB, Koffijberg H, Coupé VMH. Choosing a Metamodel of a Simulation Model for Uncertainty Quantification. Medical Decision Making. 2022 Jan 1;42(1):28–42.

9. Jalal H, Trikalinos TA, Alarid-Escudero F. BayCANN: Streamlining Bayesian Calibration With Artificial Neural Network Metamodeling. Front Physiol. 2021 May 25;12.

10. Weyant C, Brandeau ML. Personalization of Medical Treatment Decisions: Simplifying Complex Models while Maintaining Patient Health Outcomes. Medical Decision Making. 2022;42(4).

11. Malloy GSP, Brandeau ML. When Is Mass Prophylaxis Cost-Effective for Epidemic Control? A Comparison of Decision Approaches. Medical Decision Making. 2022 Nov 1;42(8):1052–63.

12. Weyant C, Lee S, Andrews JR, Alarid-Escudero F, Goldhaber-Fiebert JD. Dynamics of Respiratory Infectious Diseases in Incarcerated and Free-Living Populations: A Simulation Modeling Study. https://doi.org/101177/0272989X221115364 [Internet]. 2022 Jul 29 [cited 2023 Feb 21];43(1):42–52. Available from: https://journals.sagepub.com/doi/10.1177/0272989X221115364

13. Hauser T, Keats A, Tarasov L. Artificial neural network assisted Bayesian calibration of climate models. Clim Dyn [Internet]. 2012 Jul 22 [cited 2023 Feb 1];39(1–2):137–54. Available from: https://link.springer.com/article/10.1007/s00382-011-1168-0

14. van Ballegooijen M, Rutter CM, Knudsen AB, Zauber AG, Savarino JE, Lansdorp-Vogelaar I, et al. Clarifying differences in natural history between models of screening: The case of colorectal cancer. Vol. 31, Medical Decision Making. 2011. p. 540–9.

15. National Cancer Institute. CISNET: Colorectal Cancer Modeling [Internet]. 2022 [cited 2022 Aug 10]. Available from: https://cisnet.cancer.gov/colorectal/

16. Knudsen AB, Rutter CM, Peterse EFP, Lietz AP, Seguin CL, Meester RGS, et al. Colorectal Cancer Screening: An Updated Modeling Study for the US Preventive Services

Task Force. Vol. 325, JAMA - Journal of the American Medical Association. American Medical Association; 2021. p. 1998–2011.

17. Kleijnen JPC. Design and Analysis of Simulation Experiments. 2015 [cited 2023 Feb 2];230. Available from: https://research.tilburguniversity.edu/en/publications/design-and-analysis-of-simulation-experiments-2

18. James G, Witten D, Hastie T. Introduction to Statistical Learning with Applications in R. Vol. 11, Synthesis Lectures on Mathematics and Statistics. 2019.

19. Thiagarajan JJ, Venkatesh B, Anirudh R, Bremer PT, Gaffney J, Anderson G, et al. Designing accurate emulators for scientific processes using calibration-driven deep models. Nat Commun. 2020 Dec 1;11(1).

20. Stan Development Team. RStan: the R interface to Stan [Internet]. 2022 [cited 2022 Dec 7]. Available from: https://mc-stan.org

21. Brooks SP, Gelman A. General Methods for Monitoring Convergence of Iterative Simulations. Journal of Computational and Graphical Statistics. 1996;434–55.

22. Degeling K, IJzerman MJ, Lavieri MS, Strong M, Koffijberg H. Introduction to Metamodeling for Reducing Computational Burden of Advanced Analyses with Health Economic Models: A Structured Overview of Metamodeling Methods in a 6-Step Application Process. Medical Decision Making [Internet]. 2020 Apr 1 [cited 2023 Jan 19];40(3):348–63. Available from: https://journals.sagepub.com/doi/10.1177/0272989X20912233

23. Reiker T, Golumbeanu M, Shattock A, Burgert L, Smith TA, Filippi S, et al. Emulator-based Bayesian optimization for efficient multi-objective calibration of an individual-based model of malaria. Nat Commun. 2021 Dec 1;12(1).

24. Eason J, Cremaschi S. Adaptive sequential sampling for surrogate model generation with artificial neural networks. Comput Chem Eng. 2014 Sep 4;68:220–32.

25. Ellis AG, Iskandar R, Schmid CH, Wong JB, Trikalinos TA. Active learning for efficiently training emulators of computationally expensive mathematical models. Stat Med [Internet]. 2020 Nov 10 [cited 2023 Feb 2];39(25):3521–48. Available from: https://onlinelibrary.wiley.com/doi/full/10.1002/sim.8679

Tables

Table 1. *Transformations, structure, training, and calibration time of the ANN emulator selected for each CISNET model*

Model	Required transformation	Best out-of-sample ANN Structure	Training time	Calibration time
SimCRC *30 parameters* *110 targets*	- Scale inputs (-1 to 1) - Scale outputs (-1 to 1)	- 4 hidden layers - 360 hidden nodes - Activation function: Hyperbolic tangent	39 min	6.7 hours
MISCAN-Colon *37 parameters* *93 targets*	- Scale inputs (-1 to 1) - Scale outputs (-1 to 1)	- 4 hidden layers - 114 hidden nodes - Activation function: Hyperbolic tangent	26 min	3.6 hours
CRC-SPIN *22 parameters* *41 targets*	- Normalize inputs ~ N(0,1) - Scale outputs (-1 to 1)	- 1 hidden layer - 140 hidden nodes - Activation function: Sigmoid	10 min	0.5 hours

Figures

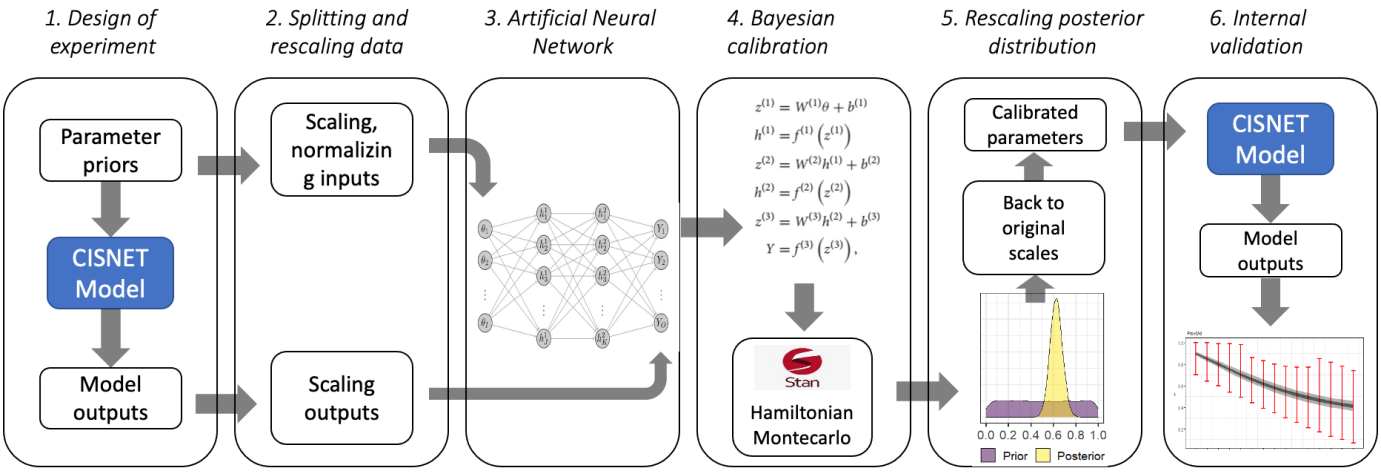

Figure 1. Diagram of BayCANN implementation

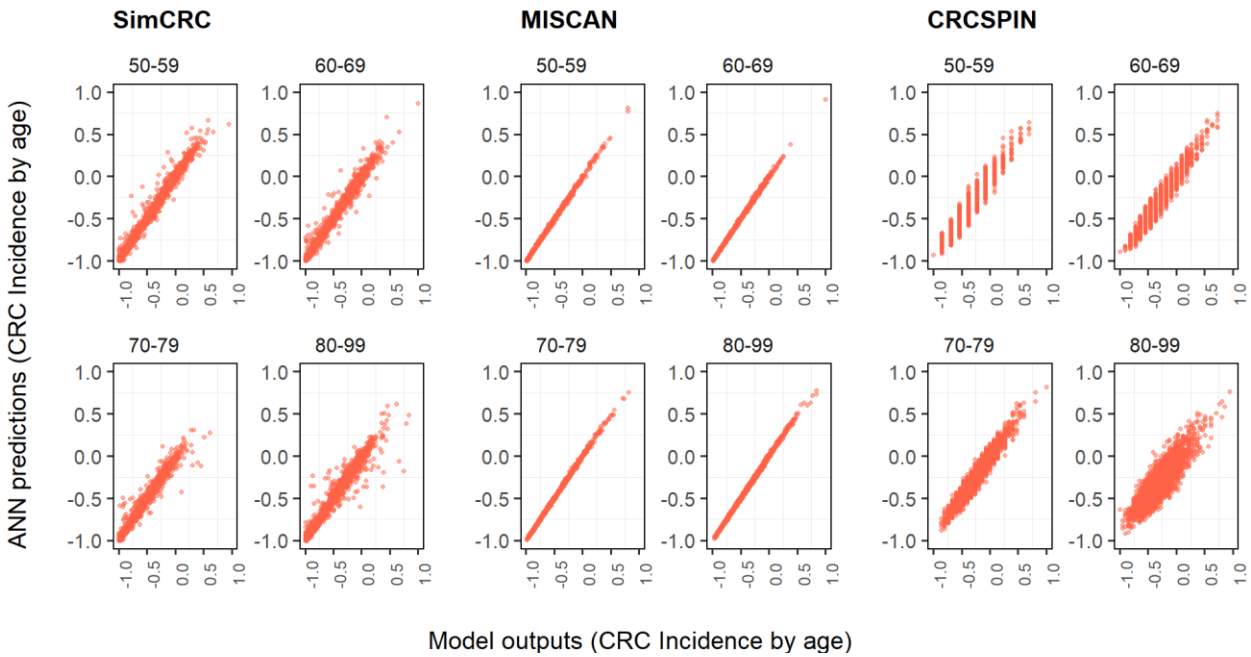

Figure 2. ANN predictions. (y-axis) vs. model outputs (x-axis) for four age groups of CRC incidence targets

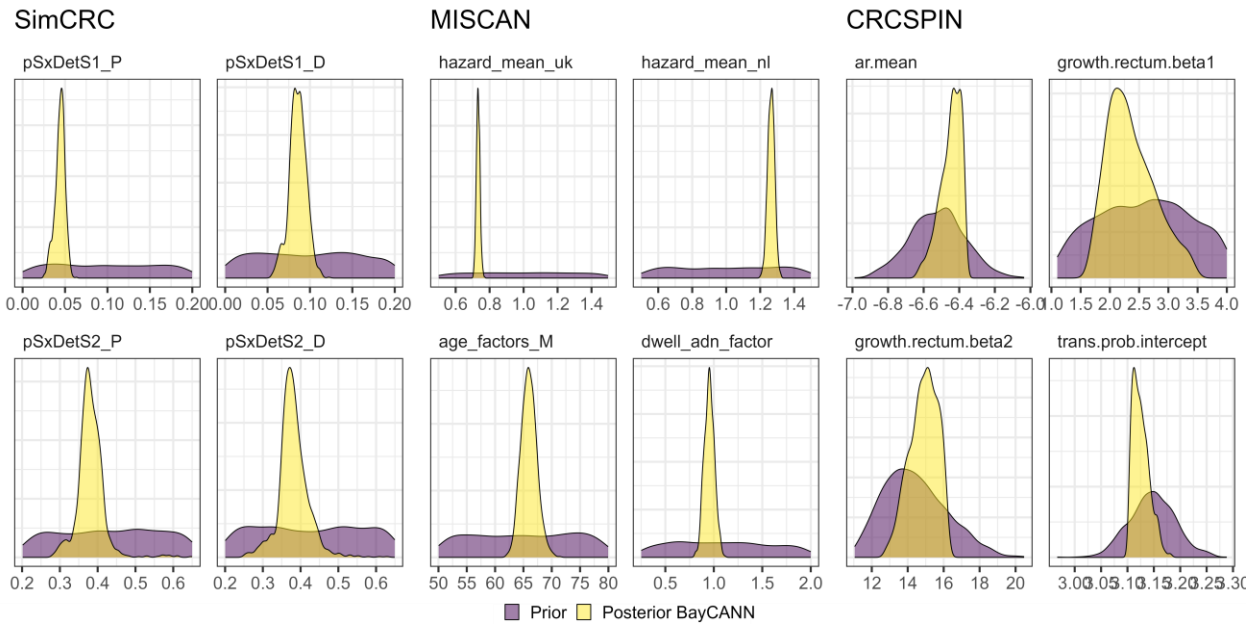

Figure 3. Prior and posterior marginal distributions of calibrated parameters for the three CISNET-CRC models

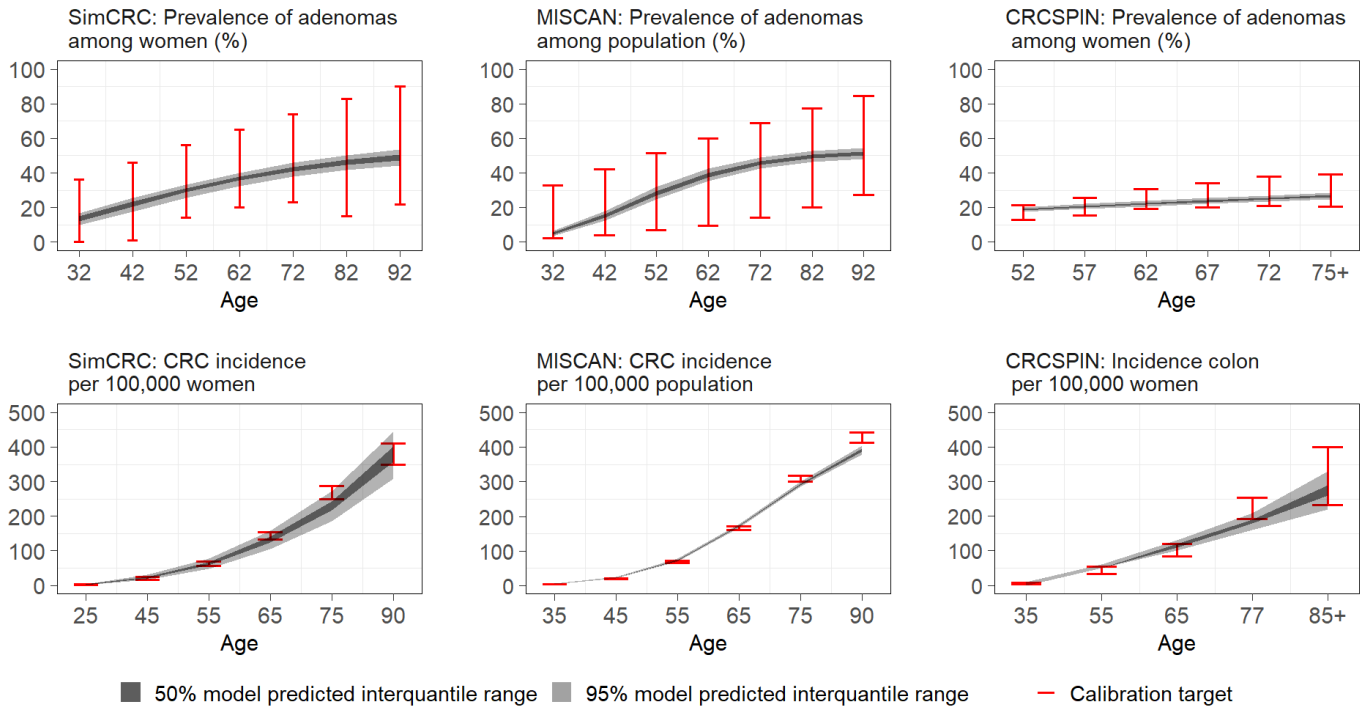

Figure 4. Validation for prevalence and incidence targets of SimCRC, MISCAN-Colon and CRC-SPIN models.